

Reduction of thermal conductance in two-dimensional phononic crystals by coherent phonon scattering

Roman Anufriev¹ and Masahiro Nomura^{1,2,*}

¹*Institute of Industrial Science, University of Tokyo, Tokyo, 153-8505, Japan*

²*Institute for Nano Quantum Information Electronics, University of Tokyo, Tokyo, 153-8505, Japan*

*Email address: nomura@iis.u-tokyo.ac.jp

The impact of lattice type, filling fraction and thickness of two-dimensional silicon phononic crystals on the reduction of thermal conductance at low temperatures is investigated systematically using the theory of elasticity and finite element method. Increase in the thickness and filling fraction of the phononic crystal affects the group velocity and phonon density of states and, as a consequence, reduce the in-plane thermal conductance of the structure as compared to unpatterned membrane. The reduction does not depend significantly on the lattice type of phononic crystals, despite the differences in symmetry and geometry. Moreover, the temperature dependence of coherent scattering is assessed, and our results demonstrate that coherent scattering plays an important role in realistic nanostructures only at relatively low temperatures.

I. INTRODUCTION

Phononic nanostructures are regarded as possible candidates for applications involving phonon management [1–3], due to the possibility to manipulate the flux of vibrational energy (i.e., heat or sound) by band engineering. Indeed, on the one hand, phononic crystals may exhibit complete phononic bandgaps, i.e., regions of frequency where the propagation of elastic waves is forbidden in any direction; the physics of this phenomenon has been investigated both theoretically [3–9] and experimentally [5,10] in various types of two-dimensional (2D) phononic crystals. On the other hand, Bragg diffraction and local resonances in the periodic media result in the flattening of branches in phonon dispersion in a wide range of frequencies. This change of phonon dispersion leads to changes of the group velocities of phonons [11–13] and the density of states (DOS) [11,13–15]. These effects originate from the wave nature of phonons and are associated with coherent scattering, which is the process when phonons preserve their phase after a scattering event, in contrast to various incoherent scattering processes when phonons do not preserve their phase. Such modifications of phonon dispersion are thought to have the ability to reduce the thermal conductivity of nanostructures, in addition to reduction by incoherent scattering mechanisms such as surface [16–18], impurity [19], and Umklapp [17,20] scattering processes. Recent experiments demonstrated very low values of thermal conductivity at room temperature in freestanding thin-film silicon nanostructures with 2D square [14,21] and hexagonal [22] arrays of holes.

To explain these low values of thermal conductivity, Dechaumphai *et al.* [12] developed a model that takes into account both coherent and incoherent scattering mechanisms, and Lacatena *et al.* [23] used a molecular dynamic approach, whereas Jain *et al.* [24] argued that coherent scattering is unlikely to appear at room temperature and some of these experimental results could be explained by treating phonons as particles with bulk properties. However, Zen *et al.* [11] demonstrated that, in 2D phononic structures, at sub-kelvin temperatures, thermal conductance is totally controlled by coherent modifications of phonon dispersion, while incoherent mechanisms play a negligible role. An overview of recent theoretical and experimental investigations shows that coherent scattering of phonons can play an important role in heat transport, while its dependence on the geometry and temperature of the structure remains a disputable matter. No systematic theoretical studies of this effect are available in the literature.

In this study, we use the theory of elasticity and finite element method (FEM) to investigate theoretically the impact of the phononic structure design on the reduction of the group velocity and DOS in the in-plane directions. We demonstrate the dependence of thermal conductance reduction on the thickness, radius-to-period ratio, and lattice type of the phononic crystal structure. Moreover, we study the temperature dependence of this effect and discuss its occurrence in realistic nanostructures at different temperatures.

II. SIMULATION OF PHONONIC CRYSTALS

We simulate infinite periodic arrays of holes in thin freestanding silicon membranes [Fig. 1(a)] with constant period ($a = 160$ nm) and various thicknesses (h) and hole radii (r). An infinite structure is simulated by considering a three-dimensional unit cell of finite thickness (h) with Floquet periodic boundary conditions applied in the x – y plane [6]. At the low temperature limit, the wavelengths of phonons are longer than the characteristic scale of the system. Thus, we can use classical elasticity theory to compute the phonon modes. We use FEM, implemented by COMSOL MULTIPHYSICS® v4.4 software, to calculate numerically the phonon dispersion $\omega(k)$ from the elastodynamic wave equation:

$$\mu \nabla^2 \mathbf{u} + (\mu + \lambda) \nabla(\nabla \cdot \mathbf{u}) = -\rho \omega^2 \mathbf{u}, \quad (1)$$

with \mathbf{u} as the displacement vector, $\rho = 2329$ kg m⁻³ as the mass density, and $\lambda = 84.5$ GPa and $\mu = 66.4$ GPa as the Lamé parameters of silicon. First we calculate the eigenfrequencies for the wave vectors at the periphery of the irreducible triangle of the first Brillouin zone (BZ) [Fig. 1(b)], and then we evaluate the eigenfrequencies in the interior of the first

BZ as an extrapolation of the values at the periphery within the triangle [Fig. 1.(c)] [25]. To study the in-plane heat transport through the structure, we calculate the heat flux spectra $Q(\omega, T)$ at a given temperature (T) as:

$$Q(\omega, T) \propto \sum_m \int_0^{FBZ} \hbar \omega_m D_m(k) |\vec{v}_m(k)| f(\omega_m, T) dk \quad (2)$$

where v_m and D_m are the group velocity and the DOS calculated with close attention to the band intersections, and f is the Bose-Einstein distribution [26]. The integrals are evaluated over the entire first BZ for each mode (m) and then summed. Figures 1(d), 1(e), and 1(f) show typical spectra of the average group velocity, DOS, and heat flux calculated from the obtained band diagram.

To verify the validity of our calculation, we simulated the same structures as those studied in the literature [4,6,12,27] and found obtained band diagrams and group velocity spectra to be in agreement with the literature. Moreover, we found good agreement with heat flux spectra and thermal conductivity results reported by Maasilta *et al.* [11,28], which proves that extrapolation of the eigenfrequencies in the interior of the first BZ and imperfection of our band sorting algorithm do not produce significant inaccuracy.

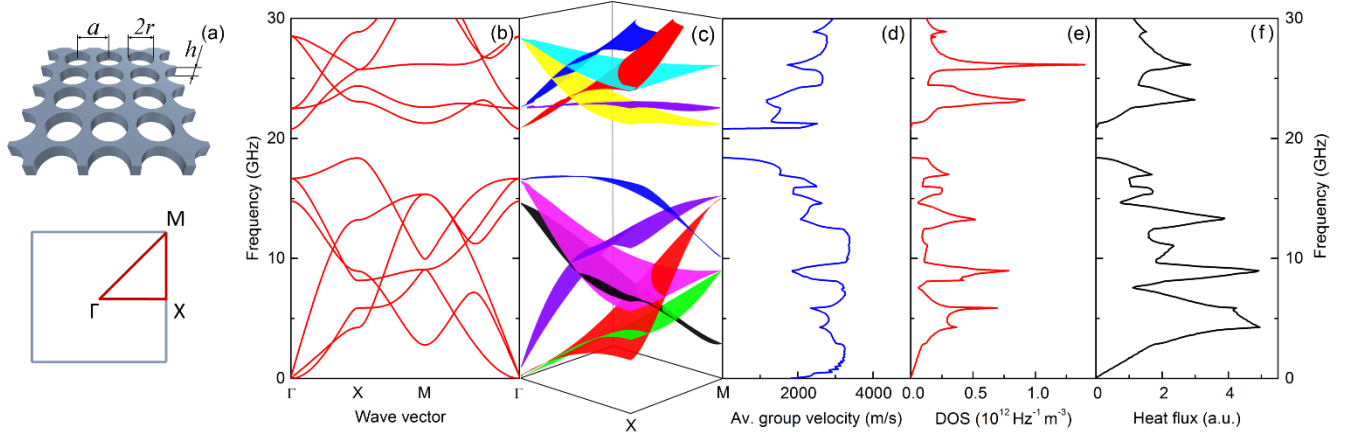


FIG. 1. (Color online) (a) Scheme of the simulated structure, its unit cell, and the first BZ with the high symmetry points: Γ (0, 0), X (π/a , 0), and M (π/a , π/a). (b) Unsorted band diagram of the structure with $a = 160$ nm, $r/a = 0.45$, and $h = 80$ nm plotted at the high symmetry points. (c) Sorted band diagram plotted in the interior of the irreducible triangle of the first BZ. Spectra are shown for (d) the average group velocity, (e) DOS, and (f) heat flux.

III. IMPACT OF THE DESIGN

We study three types of lattice: square, hexagonal [Fig. 2(a)], and honeycomb [Fig. 2(b)]. Figures 2(c) and 2(d) show the corresponding phonon dispersions of hexagonal and honeycomb lattices, respectively.

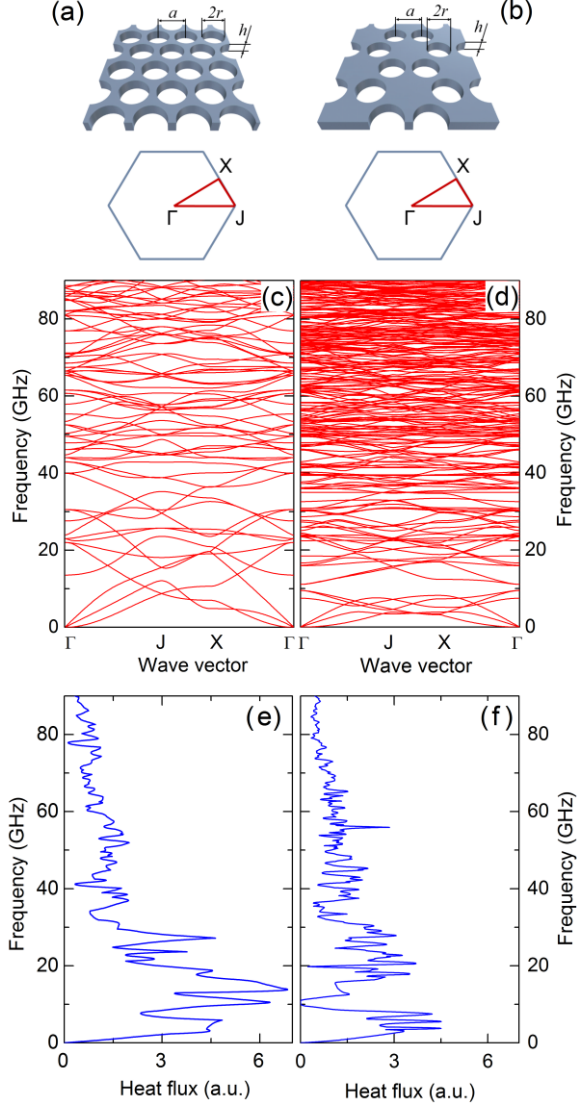


FIG. 2. (Color online) Schemes of the structures and first BZs with high symmetry points for (a) hexagonal lattice: Γ (0, 0), J ($4\pi/3a$, 0), and X (π/α , $\pi/\sqrt{3}a$), and (b) honeycomb lattices: Γ (0, 0), J ($4\pi/3\sqrt{3}a$, 0), and X ($\pi/\sqrt{3}a$, $\pi/\sqrt{3}a$). The band diagrams are shown for (c) hexagonal and (d) honeycomb structures ($r/a = 0.45$, $a = 160$ nm, and $h = 80$ nm), and (e, f) the corresponding spectra of heat flux at 1 K.

Despite the similarities between the lattices, the band diagrams are completely different. However, the corresponding spectra of the heat flux are quite similar, as shown in Figs. 2(e) and 2(f). This shows that density of bands in band

diagrams does not reflect heat transport properties. Analyzing the appearance of the phononic bandgap in the different lattices, we found the same trends as those known from the literature [4,8,9,11,27,29]: the width of the bandgap increases as a function of the r/a ratio, and the widest bandgap is expected for the honeycomb lattice, while, as a function of the h/a ratio, the widest bandgaps are expected at around the values of 0.5 and 1. However, the bandgap alone may play only a minor role in the suppression of thermal conductance at temperatures above the sub-kelvin range, as is evident from the heat flux spectrum at 1 K [Fig. 2(f)]: the region covered by the bandgap is very small, as compared to the whole range of frequencies. For this reason, we focus our study on the changes in the group velocity and DOS.

To illustrate how coherent modifications of phonon dispersion impact heat transport, we consider two square lattice nanostructures with the same thickness ($h = 80$ nm) and period ($a = 160$ nm), but different r/a ratios (0.2 and 0.45). Figure 3(a) demonstrates that both phononic structures show significant reduction of the group velocity, as compared to the unpatterned membrane, but this reduction is larger in the structure with larger radius ($r/a = 0.45$ nm). This reduction is a direct consequence of band flattening in phononic crystals [11,12,30]. The DOS of the phononic structures are similar to that of the membrane. Yet again, the structure with $r/a = 0.45$ demonstrates a lower DOS [Fig. 3(b)]. As a consequence, the heat flux, which is proportional to the product of the group velocity and DOS, shows a reduction for both phononic structures, as compared to the membrane, except for the low frequency part [13] [Fig. 3(c)]. This reduction is stronger in the structure with a larger radius-to-period ratio, due to the reduction in DOS spectrum. The same reduction is observed also in hexagonal and honeycomb lattices. This result is consistent with recent experimental and theoretical data where the heat flux in SiN phononic structures was also significantly reduced [11].

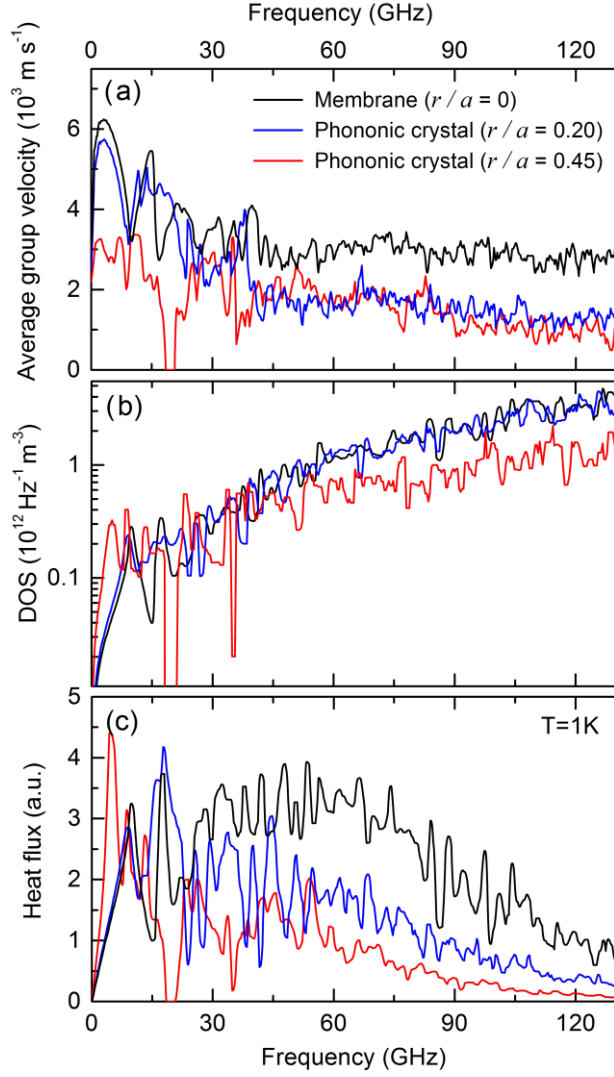


FIG. 3. (Color online) Spectra of (a) the average group velocity, (b) the DOS, and (c) the heat flux at 1 K, calculated for the membrane (black) and square lattice phononic structures with periods $r/a = 0.2$ (blue) and $r/a = 0.45$ (red), and $a = 160 \text{ nm}$ for both structures. The thickness of all structures is $h = 80 \text{ nm}$. The curves are smoothed for clarity.

To compare quantitatively structures with different designs, we evaluate the thermal conductance of the structure as [11]:

$$G(T) \propto \frac{1}{2\pi^2} \sum_m \int_0^{FBZ} \hbar \omega_m \left| \frac{d\omega_m}{d\vec{k}} \right| \left| \frac{\partial f(\omega, T)}{\partial T} \right| d\vec{k} \quad (3)$$

In this work we mostly consider $G_{PnC} / G_{Membrane}$ ratio, where G_{PnC} and $G_{Membrane}$ are the thermal conductance of phononic crystals and a membrane, respectively, calculated using a unit cell of the same shape, size and thickness. Figure 4 shows relative thermal conductance in phononic structures of different designs. All three lattices demonstrate the same

decreasing trend as a function of the r/a ratio [Fig. 4(a)]. This fact is mostly explained by the reduction of group velocity due to the band flattening as the hole size is increased [12], though the reduction of DOS at high frequencies also play a role. Therefore, the strongest reduction of thermal conductance takes place in the structures with the highest r/a ratio possible, since it is optimal for both coherent and incoherent [16,18,24] scattering mechanisms. This conclusion is also supported by recent molecular dynamics calculations [23].

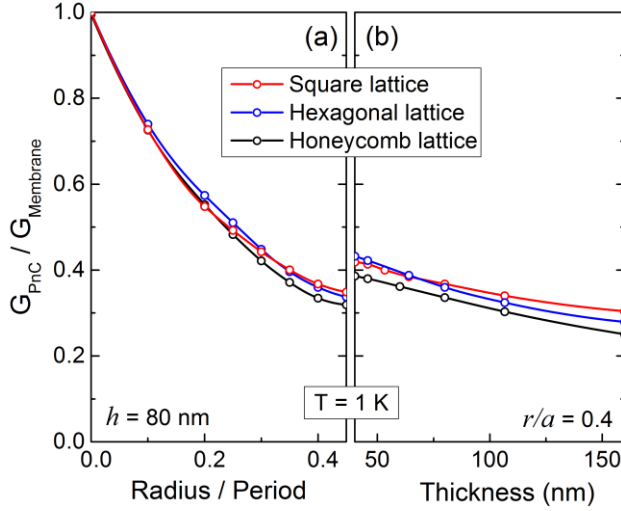


FIG. 4. (Color online) Relative thermal conductance in phononic structures with square (black), hexagonal (red), and honeycomb (blue) lattices ($a = 160 \text{ nm}$), calculated at 1 K as (a) a function of r/a ratio, with constant thickness ($h = 80 \text{ nm}$), and (b) a function of the thickness with constant $r/a = 0.4$.

Next, we study the dependence of thermal conductance on the thickness of the structures. For the unpatterned membranes this dependence has been investigated by Maasilta et al. [28,31]. Here we study the thickness dependence of the thermal conductance reduction by phononic crystals. Counterintuitively, we found that this reduction is larger in thicker structures. The actual values of thermal conductance in both phononic crystals and membranes are increasing with thickness, but the $G_{p\text{n}C} / G_{\text{Membrane}}$ ratio is slightly decreasing, as shown in Figure 4(b).

As far as different lattices are concerned, structures with the same radius, period and thickness, but different lattice type, always demonstrate a very similar reduction of thermal conductance [Fig. 4]. This fact might be related to the presence of local resonances which, probably being similar in different lattices, partly can form the dispersion of the structures [6]. However, this finding implies that the choice of the lattice type can be made in order to achieve the best mechanical or electrical properties or the strongest incoherent surface scattering.

IV. TEMPERATURE DEPENDENCE

Since thermal conductance depends on the Bose–Einstein distribution, its reduction in phononic crystals can be affected by temperature. Indeed, Figure 5(a) shows that reduction of thermal conductance in phononic crystals is temperature dependent, at least at low temperatures. At the low temperature limit, the thermal conductance of phononic crystals approaches, and even overcomes, that of the membrane (i.e. $G_{PnC} / G_{Membrane} > 1$). This reflects the thermal conductance boost effect [13]: at the temperatures about 0.1 K, only few first bands are occupied, and these bands in phononic crystals have DOS higher than that in membrane [Fig 3(b)], while the reduction of group velocity in this region is moderate [Fig 3(a)]. However, as the temperature is increased, the reduction of thermal conductance also is increased towards certain limit (≈ 0.24 for $r/a = 0.4$). This saturation takes place due to the occupation of higher-frequency states at higher temperatures. Indeed, at higher frequencies the values of the group velocity and DOS in phononic crystals are reduced by some value which is nearly constant over wide range of high frequencies (see Fig 3(a) at the frequencies > 60 GHz), so the reduction of thermal conductance reaches its maximum.

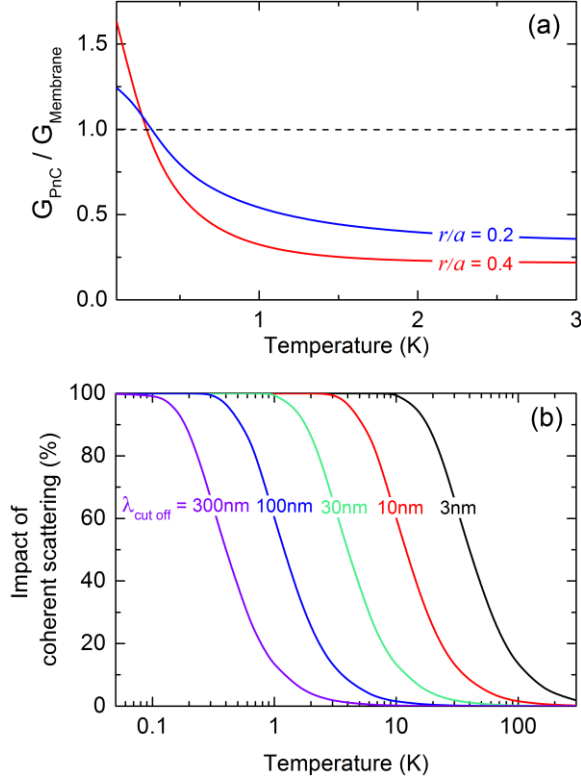


FIG. 5. (Color online) (a) Relative thermal conductance in square lattice phononic structures ($h = 80$ nm, $a = 160$ nm) with different $r/a = 0.2$ (blue) and 0.4 (red) as a function of temperature. (b) Portion of thermal conductance ($P_{coherent}$)

impacted by coherent scattering in square lattice phononic crystals ($h = 80$ nm, $r/a = 0.4$, $a = 160$ nm) as a function of temperature for different values of the cutoff wavelength.

On the other hand, the wave picture of phonons, discussed in this work, is relevant probably only at relatively low temperatures, when the thermal phonon wavelengths are comparable to the characteristic size of the structure [11,12,24]. Indeed, at room temperature, the phonon wavelength is in the 1–5 nm range [32], which is comparable to the surface roughness, so the phonon boundary scattering is mostly incoherent (or diffusive) [24], and wave interference cannot develop; at low temperatures, thermal phonon wavelengths become longer, and coherent phonon scattering may not only play an important role, but even fully control the phonon transport [11].

To discuss the role of coherent scattering at different temperatures, we assume the existence of a cutoff wavelength (λ_{cutoff}) below which phonon scattering is purely incoherent [12]. Such a cutoff wavelength is assumed typically to be at least bigger than the surface roughness. Moreover, according to the formula of Ziman [33]: $p = \exp(-16\pi^3\delta^2/\lambda^2)$, the wavelength (λ) should be at least of the order of 100 nm to achieve a specularity (p) of 0.5, for a surface roughness (δ) of a few nanometers. In phononic nanostructures, the cutoff wavelength is often approximated by the characteristic size of the structure, which is the period [24] or neck size [12,34] of the phononic crystal. To estimate the part of heat affected by coherent scattering, we calculate the ratio of the part of the heat flux spectrum up to λ_{cutoff} to the entire spectrum (Eq. 3). Here, to obtain the heat flux at high temperatures, we approximate the group velocity and DOS by linear fits and extend them to high frequencies.

$$P_{coherent}(T) = \frac{\int_0^{\lambda_{cutoff}} Q(\lambda, T) d\lambda}{\int_0^{\infty} Q(\lambda, T) d\lambda} \quad (3)$$

Figure 5(b) shows the impacted portion of the heat flux ($P_{coherent}$) as a function of temperature for different values of the cutoff wavelength (λ_{cutoff}). These data demonstrate that, in structures with $\lambda_{cutoff} > 100$ nm, coherent scattering significantly impacts the thermal conductance only at temperatures of about 1 K. This finding is in agreement with the experimental observations reported by Zen *et al.* [11] where the thermal conductance starts to deviate from a completely coherent picture above 0.4 K. At room temperature, a noticeable impact can be produced only by structures with λ_{cutoff} shorter than a few nanometers, which implies unrealistic conditions of very small characteristic sizes and/or the absence of surface

roughness. These estimations of the impact of coherent scattering are in agreement with similar considerations involving the random path tracing method [34]. Therefore, at room temperature, coherent scattering probably plays a much less important role than other scattering mechanisms. Thus, the applications of coherent phonon control in phononic crystals are probably limited to low-temperature devices such as transition edge sensors [28].

V. CONCLUSION

We have investigated the impact of structure design on the efficiency of coherent phonon scattering in 2D phononic crystals. Our results demonstrate that the reduction of thermal conductance by phononic nano-patterning is increasing as a function of the thickness and radius-to-period ratio, at least as far as constant period is concerned. However, thermal conductance reduction does not depend on the lattice type, despite differences in symmetry and geometry. Therefore, the lattice choice can be made to ensure strong incoherent scattering (hexagonal lattice) or rigidity of the structure (honeycomb lattice). Our study also demonstrates that the reduction of thermal conductance is temperature dependent and reaches its maximum only at certain temperature, yet coherent scattering plays an important role in realistic nanostructures only at relatively low temperatures.

ACKNOWLEDGMENTS

This work was supported by the Project for Developing Innovation Systems of the Ministry of Education, Culture, Sports, Science and Technology (MEXT), Japan and by KAKENHI (25709090 and 15K13270).

REFERENCES

- [1] G. Schierning, *Phys. Status Solidi* **211**, 1235 (2014).
- [2] M. Maldovan, *Nature* **503**, 209 (2013).
- [3] J. Gomis-Bresco, D. Navarro-Urrios, M. Oudich, S. El-Jallal, A. Griol, D. Puerto, E. Chavez, Y. Pennec, B. Djafari-Rouhani, F. Alzina, A. Martínez, and C. M. S. Torres, *Nat. Commun.* **5**, 4452 (2014).
- [4] J. O. Vasseur, P. A. Deymier, B. Djafari-Rouhani, Y. Pennec, and A.-C. Hladky-Hennion, *Phys. Rev. B* **77**, 085415 (2008).
- [5] Y. Pennec, J. O. Vasseur, B. Djafari-Rouhani, L. Dobrzański, and P. A. Deymier, *Surf. Sci. Rep.* **65**, 229 (2010).
- [6] R. Pourabolghasem, A. Khelif, S. Mohammadi, A. A. Eftekhar, and A. Adibi, *J. Appl. Phys.* **116**, 013514 (2014).

- [7] D. Feng, D. Xu, G. Wu, B. Xiong, and Y. Wang, *Appl. Phys. Lett.* **103**, 151906 (2013).
- [8] Y. Pennec, B. Djafari Rouhani, E. H. El Boudouti, C. Li, Y. El Hassouani, J. O. Vasseur, N. Papanikolaou, S. Benchabane, V. Laude, and A. Martinez, *Opt. Express* **18**, 14301 (2010).
- [9] S. Sadat-Saleh, S. Benchabane, F. I. Baida, M.-P. Bernal, and V. Laude, *J. Appl. Phys.* **106**, 074912 (2009).
- [10] S. Mohammadi, A. A. Eftekhar, A. Khelif, W. D. Hunt, and A. Adibi, *Appl. Phys. Lett.* **92**, 221905 (2008).
- [11] N. Zen, T. A. Puurinen, T. J. Isotalo, S. Chaudhuri, and I. J. Maasilta, *Nat. Commun.* **5**, 3435 (2014).
- [12] E. Dechaumphai and R. Chen, *J. Appl. Phys.* **111**, 073508 (2012).
- [13] R. Anufriev and M. Nomura, *Phys. Rev. B* **91**, 245417 (2015).
- [14] P. E. Hopkins, C. M. Reinke, M. F. Su, R. H. Olsson, E. A. Shaner, Z. C. Leseman, J. R. Serrano, L. M. Phinney, and I. El-Kady, *Nano Lett.* **11**, 107 (2011).
- [15] B. L. Davis and M. I. Hussein, *Phys. Rev. Lett.* **112**, 055505 (2014).
- [16] M. Nomura, J. Nakagawa, Y. Kage, J. Maire, D. Moser, and O. Paul, *Appl. Phys. Lett.* **106**, 143102 (2015).
- [17] W. Fon, K. C. Schwab, J. M. Worlock, and M. L. Roukes, *Phys. Rev. B* **66**, 045302 (2002).
- [18] M. Nomura, Y. Kage, J. Nakagawa, T. Hori, J. Maire, J. Shiomi, R. Anufriev, D. Moser, and O. Paul, *Phys. Rev. B* **91**, 205422 (2015).
- [19] A. I. Hochbaum, R. Chen, R. D. Delgado, W. Liang, E. C. Garnett, M. Najarian, A. Majumdar, and P. Yang, *Nature* **451**, 163 (2008).
- [20] Y.-J. Han, *Phys. Rev. B* **54**, 8977 (1996).
- [21] J.-K. Yu, S. Mitrovic, D. Tham, J. Varghese, and J. R. Heath, *Nat. Nanotechnol.* **5**, 718 (2010).
- [22] J. Tang, H.-T. Wang, D. H. Lee, M. Fardy, Z. Huo, T. P. Russell, and P. Yang, *Nano Lett.* **10**, 4279 (2010).
- [23] V. Lacatena, M. Haras, J.-F. Robillard, S. Monfray, T. Skotnicki, and E. Dubois, *Appl. Phys. Lett.* **106**, 114104 (2015).
- [24] A. Jain, Y.-J. Yu, and A. J. H. McGaughey, *Phys. Rev. B* **87**, 195301 (2013).
- [25] K. Busch and S. John, *Phys. Rev. E* **58**, 3896 (1998).
- [26] A. Majumdar, *J. Heat Transfer* **115**, 7 (1993).
- [27] S. Mohammadi, A. A. Eftekhar, A. Khelif, H. Moubchir, R. Westafer, W. D. Hunt, and A. Adibi, *Electron. Lett.* **43**, 898 (2007).
- [28] I. J. Maasilta and T. Kühn, *J. Low Temp. Phys.* **151**, 64 (2008).
- [29] M. Maldovan and E. L. Thomas, *Appl. Phys. Lett.* **88**, 251907 (2006).
- [30] M. Nomura and J. Maire, *J. Electron. Mater.* **44**, 1426 (2014).

- [31] T. Kühn and I. J. Maasilta, Nucl. Instruments Methods Phys. Res. Sect. A Accel. Spectrometers, Detect. Assoc. Equip. **559**, 724 (2006).
- [32] K. Esfarjani, G. Chen, and H. T. Stokes, Phys. Rev. B **84**, 085204 (2011).
- [33] J. M. Ziman, *Electrons and Phonons: The Theory of Transport Phenomena in Solids* (Clarendon, Oxford, 1962).
- [34] A. M. Marconnet, T. Kodama, M. Asheghi, and K. E. Goodson, Nanoscale Microscale Thermophys. Eng. **16**, 199 (2012).